Small condensation nuclei must be present for the formation of cloud droplets. Such nuclei come from many sources, such as ocean salt, dust from clay soils, industrial combustion products, and volcanoes, and they range in size from 0.1 μ to 10 μ. Cloud droplets originally average 0.01 mm in diameter, and it is only when they exceed 0.5 mm that significant precipitation occurs. It may take hours for a small raindrop (1 mm) to grow on a condensation nucleus. As vapor-laden air rises, it cools as it expands, and as saturation occurs, water vapor begins to condense on the most active nuclei. The principal mechanism for the supply of water to the growing droplet in early stages is diffusion of water-vapor molecules down the vapor-pressure gradient toward the droplet surface. As the droplets increase in mass, they begin to move relative to the overall cloud. However, other processes must support the growth of droplets of sufficient size (0.5–3.0 mm) to overcome air resistance and to fall as precipitation. These include the coalescence process and the ice-crystal process.

The **coalescence process** is considered dominant in summer shower precipitation. As water droplets fall, the smaller ones are overtaken by larger ones, and droplet size is increased through collision. This can produce significant precipitation, especially in warm cumulus clouds in tropical regions. The **ice-crystal process** attracts condensation on freezing nuclei because of lower vapor pressures. The ice crystals grow in size through contact with other particles, and collisions cause snowflakes to form. Snowflakes may change into rain droplets after entering air in which the temperature is above freezing. Snowfall and snowmelt processes are presented in detail in Chapter 2.

Condensation nuclei can be artificially supplied to clouds to induce precipitation under certain conditions. Dry ice and silver iodide have been used as artificial nuclei. Research is continuing in this phase of weather control, and many legal and technical problems remain to be resolved regarding artificial inducement of precipitation. More discussion can be found in any standard meteorology text or on many available websites.

1.4 PRECIPITATION

Point Measurement

Considerable amounts of precipitation data are available from the NWS, the USGS, and various local governmental agencies. A number of useful websites for precipitation data are listed in Appendix E and on the textbook website http://hydrology.rice.edu/bedient/. Interpretation of national networks of rainfall data shows extreme variability in space and time, as can be seen in Figs. 1–5a and 1–5b. The main source of moisture for annual rainfall totals is evaporation from the oceans; thus precipitation tends to be heavier near the coastlines, with distortion due to orographic effects—that is, effects of changes in elevation over mountain ranges. In general, amount and frequency of precipitation is greater on the windward side of mountain barriers (the western side for the United States) and less on the lee side (eastern side), also shown in Fig. 1–5a.

Time variation of precipitation occurs seasonally or within a single storm, and distributions vary with storm type, intensity, duration, and time of year. Prevailing winds and relative temperature of land and proximity of bordering

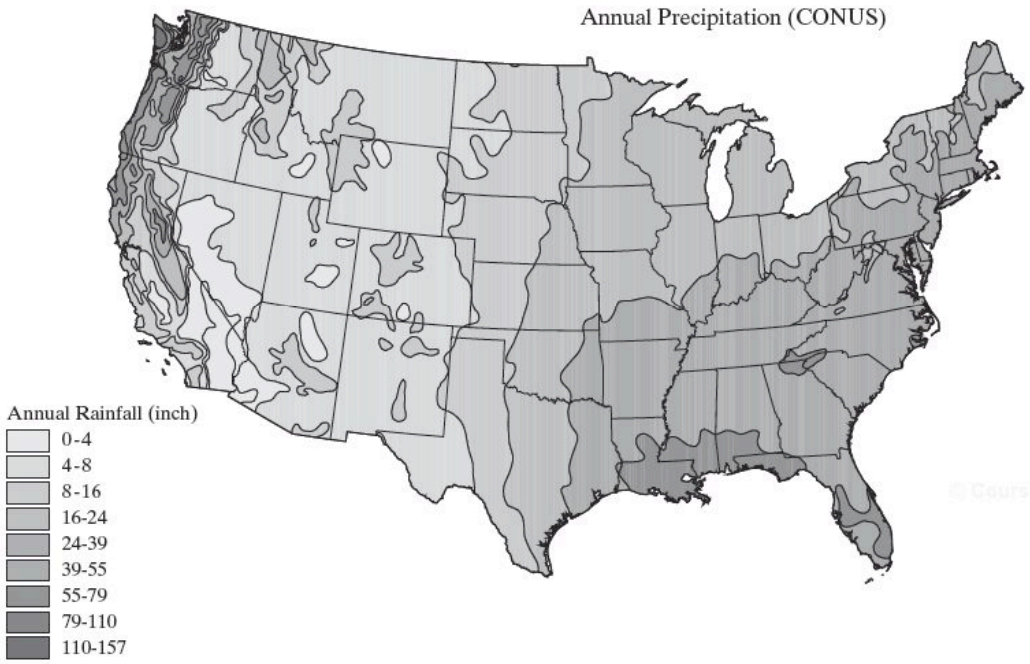

Figure 1–5a
Distribution of average annual precipitation.

ocean have an effect. One interesting statistic is the maximum recorded rainfall that can occur at a single gage. These data are shown for eight major U.S. cities in Table 1–3. Totals for a 24-hour period, for example, range from a low of 4.67 in. (119 mm) in San Francisco to a high of 43 in. (1092 mm) in Alvin near Houston, TX, indicating the wide range that can occur. Much larger values near the Gulf coast reflect the impact of severe storms and hurricanes. World precipitation records, shown in Table 1–4, clearly indicate the effect of proximity to major oceans, as in the case of India.

Seasonal or monthly distributions for the United States are shown in Fig. 1–5b, where it is clear that areas such as Florida, California, and the Pacific Northwest have significant seasonal rainfall patterns compared to most areas in the country and along the eastern seaboard. Also, the west and southwest are significantly drier than the east or northwest. But the values shown are deceptive in that high-intensity thunderstorms or hurricanes can produce 15 to 30 in. of rainfall in a matter of days along the Gulf and Atlantic coasts. For example, Oregon and Washington receive most of their rainfall in the winter from fronts that move across the area, whereas in Florida thunderstorms and hurricanes produce large summer totals. Southern California, where most of the population resides, gets significantly less rainfall than the northern part. This difference in available water led to the building of the California Water Project, which transports water hundreds of miles from the reservoirs in the north to the Los Angeles area.

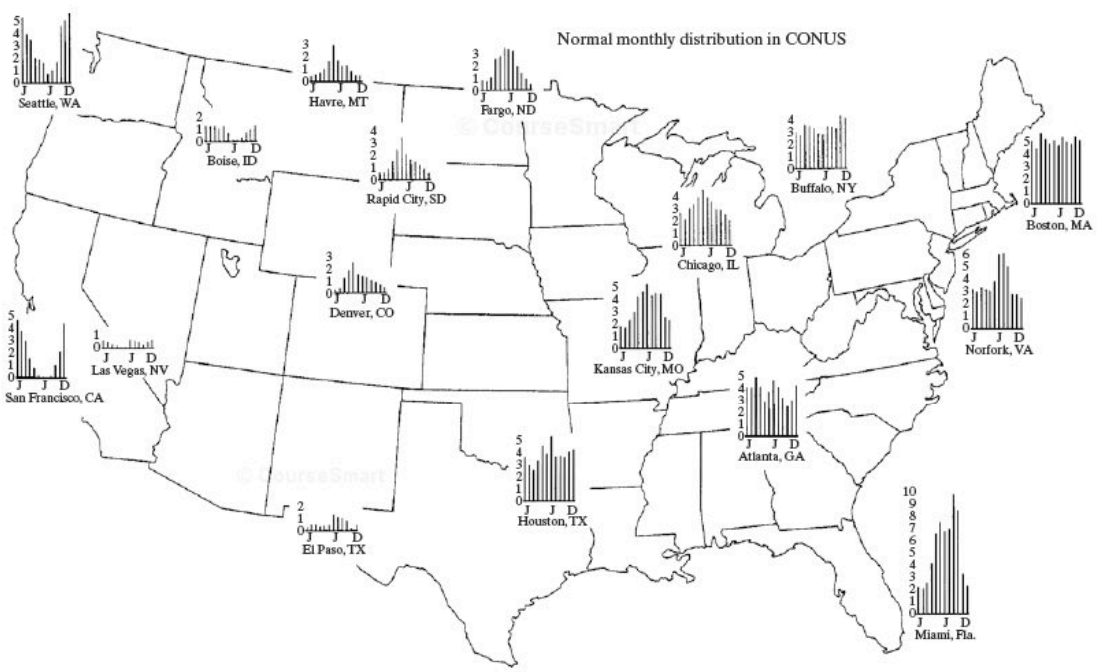

Figure 1–5b
Normal monthly distribution of precipitation in the United States (in.) (1 in. = 25.4 mm). (U.S. Environmental Data Service.)

Table 1–3. Maximum Recorded Rainfall Across the United States (in.)

	Duration		
	1 hr	6 hr	24 hr
San Francisco, CA	1.07	2.34	4.67
Portland, OR	1.31	—	7.66
Denver, CO	2.20	2.91	6.53
St. Louis, MO	3.47	5.82	8.78
New Orleans, LA	4.71	8.62	14.01
Alvin, TX (near Houston)	4.00	15.67	43.00
New York, NY	2.97	4.44	9.55
Miami, FL	4.53	10.64	15.10

Table 1–4. World Record Rainfalls

Duration	in.	mm	Location
1 min	1.50	38	Barot, Guadeloupe
8 min	4.96	126	Fussen, Bavaria
15 min	7.80	198	Plumb Point, Jamaica
20 min	8.10	206	Cutea de Arges, Rumania
42 min	12.00	305	Holt, MO
2 hr 10 min	19.00	483	Rockport, WV
4 hr 30 min	30.80	782	Smetport, PA
9 hr	42.79	1087	Belouve, Reunion
12 hr	52.76	1340	Belouve, Reunion
24 hr	73.62	1870	Ciliaos, Reunion
2 days	98.42	2500	Ciliaos, Reunion
3 days	127.56	3240	Ciliaos, Reunion
4 days	146.50	3721	Cherrapunji, India
5 days	151.73	3854	Ciliaos, Reunion
6 days	159.65	4055	Ciliaos, Reunion
7 days	161.81	4110	Ciliaos, Reunion
15 days	188.88	4798	Cherrapunji, India
1 mo	366.14	9300	Cherrapunji, India
2 mo	502.63	12,767	Cherrapunji, India
3 mo	644.44	16,369	Cherrapunji, India
6 mo	884.03	22,454	Cherrapunji, India
1 yr	1041.78	26,461	Cherrapunji, India
2 yrs	1605.05	40,768	Cherrapunji, India

Hourly or even more detailed variations of rainfall [see Fig. 1–6(a)] are often important for planning water resource projects, especially urban drainage systems. The intensity and duration of rainfall events are important in determining the hydrologic response for a watershed. Such data are available only from sophisticated rainfall recording networks, usually located in larger urban areas and along major river basins. Rainfall gage networks are maintained by the NWS, the USGS, and local county flood control districts

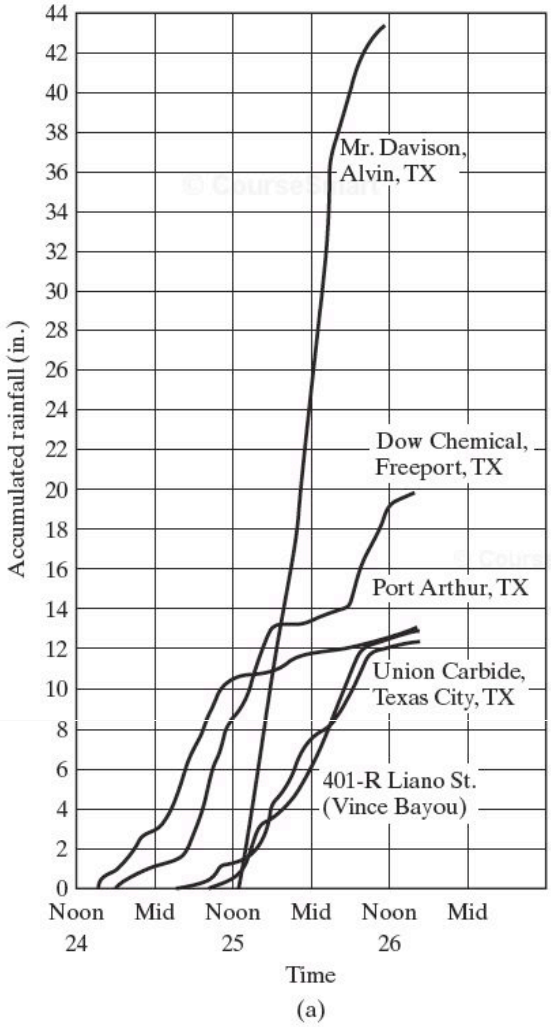

Figure 1–6a
Storm event near Houston, Texas. (a) Accumulated rainfall, July 24–26, 1979.

and utilities. An excellent source of rainfall data is now available on specific websites, such as National Climatic Data Center (NCDC) and NWS (see Appendix E).

Rainfall gages may be of the recording (Fig. 1–7) or nonrecording type, but recording gages are required if the time distribution of rainfall is desired, as is often the case for urban drainage or flood control works. The recording gage operates from a small tipping bucket that records on a strip chart, or data logger, every 0.1 or 0.01 in. of rainfall (or 0.1 or 1 mm in Canada). The data are displayed in a form shown in Fig. 1–6(a) as a **cumulative mass curve** and can be readily interpreted for total volume and intensity variations. Observers usually report daily or 12-hr amounts of rainfall (in. or mm) for nonrecording gages, providing little information on intensity.

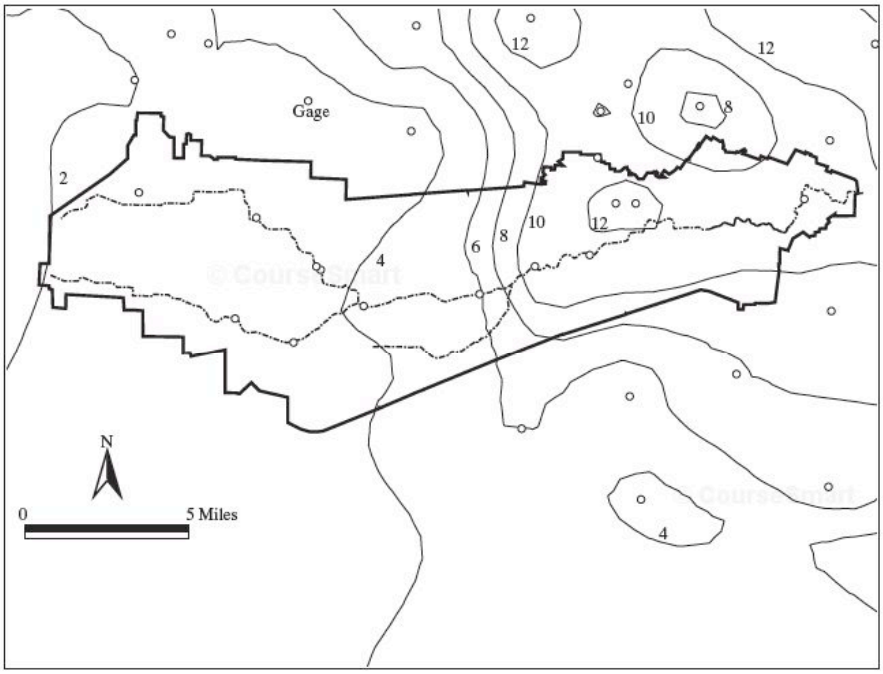

(b)

Figure 1–6b
T. S. Allison 9 hr rainfall (in.) gage contours—Brays Bayou Watershed in Houston, TX.

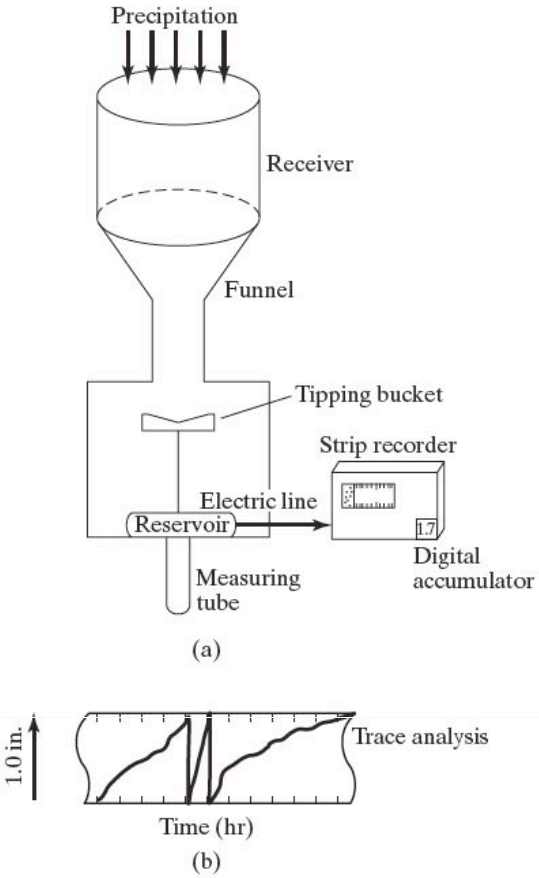

Figure 1–7
Recording tipping bucket gage. Trace returns to zero after each inch of rainfall. The slope of the trace registers intensity (in./hr).

A network of five to ten gages per 100 mi^2 is usually required in urban areas to define rainfall variability. Such networks are expensive to maintain, and any equipment failures can negate portions of the network for a given storm event. Recording rainfall gages are often located adjacent to streamflow gages, which are discussed further in Section 1.6. Temporal and areal variations in rainfall are important in determining overall hydrologic response and are discussed in more detail below.

Point rainfall can be plotted as accumulated total rainfall or as rainfall intensity at a particular gage. The first plot is referred to as a cumulative mass curve [Fig. 1–6(a)], which can be analyzed for a variety of storms to determine the frequency and character of rainfall at a given site. A **hyetograph** is a plot of rainfall intensity (in./hr) versus time, and one is depicted in Example 1–3 along with cumulative mass curves for total rainfall. Hyetographs are often used as input to hydrologic computer models for predicting watershed response to input rainfall.

EXAMPLE 1–3 **HYETOGRAPHS AND CUMULATIVE PRECIPITATION**

Table E1–3 is a record of precipitation from a recording gage for a storm in Texas, for the period between midnight and 11:15 A.M. on the same day. For the data given, develop the rainfall hyetographs and mass curves. Find the maximum-intensity rainfall for the gage in in./hr.

Table E1–3. Rainfall Data from a Recording Gage

Time (hr)	Gage Rainfall (in.)	Gage Intensity (in./hr)	Time (hr)	Gage Rainfall (in.)	Gage Intensity (in./hr)
0	0	0	5.75	3.78	0.24
0.25	0.02	0.08	6	3.84	0.24
0.5	0.07	0.2	6.25	3.9	0.24
0.75	0.4	1.32	6.5	3.95	0.2
1	0.55	0.6	6.75	4.1	0.6
1.25	0.6	0.2	7	4.3	0.8
1.5	0.62	0.08	7.25	4.93	2.52
1.75	0.62	0	7.5	5.4	1.88
2	0.82	0.8	7.75	5.61	0.84
2.25	0.88	0.24	8	5.77	0.64
2.5	0.92	0.16	8.25	6.17	1.6
2.75	1.06	0.56	8.5	6.22	0.2
3	1.1	0.16	8.75	6.27	0.2
3.25	1.47	1.48	9	6.29	0.08
3.5	1.87	1.6	9.25	6.3	0.04
3.75	2.32	1.8	9.5	6.31	0.04
4	3.1	3.12	9.75	6.32	0.04
4.25	3.4	1.2	10	6.33	0.04
4.5	3.48	0.32	10.25	6.34	0.04
4.75	3.54	0.24	10.5	6.35	0.04
5	3.62	0.32	10.75	6.36	0.04
5.25	3.68	0.24	11	6.37	0.04
5.5	3.72	0.16	11.25	6.38	0.04

SOLUTION

To plot the hyetograph for a gage, we subtract the measurement for each time period from that of the previous time period, and divide by the time step to compute intensity as shown in the table. Because the data are given as a cumulative reading, the mass curves are simply a plot of the data as given (see Fig. E1–3).

The maximum intensity for the gage occurred around 4:00 A.M.

$$\frac{(3.1 - 2.32)\text{ in.}}{0.25\text{ hr}} = 3.12\text{ in./hr}$$

This maximum intensity appears as the tallest bar on the hyetograph and as the region of greatest slope on the cumulative precipitation curve. This

Figure E1–3

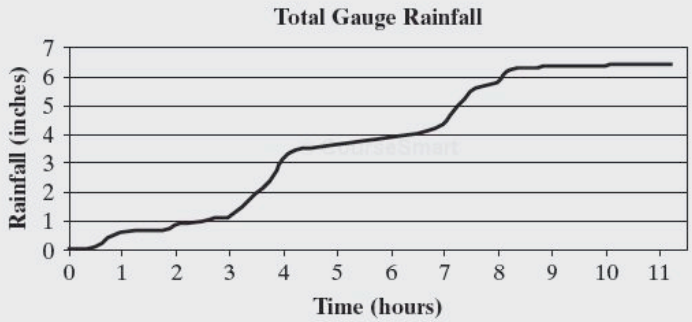

(a)

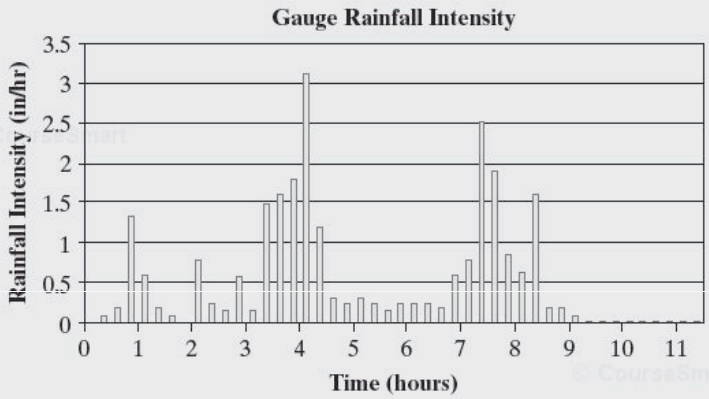

(b)

illustrates that the mass curve is the integral of the hyetograph, as, in probability theory, the cumulative distribution function is the integral of the probability density function. Note that the gage had two distinct periods of intense rainfall. These periods of rainfall intensity have the capacity to produce significant runoff and flooding.

Statistical methods (Chapter 3) can be applied to a long time series of rainfall data. For example, rainfalls of various duration ranging from 5 min to 24 hr can be analyzed to develop an estimate of, for example, the 100-yr frequency event. These data are fitted with a contour line to form one of the curves on the **intensity–duration–frequency** (IDF) curves in Fig. 1–8. Other IDF probability lines are derived in a similar fashion for the 2-yr, 5-yr, 10-yr, 25-yr, and 50-yr design rainfalls. It should be noted that IDF curves do not represent the time history of actual storms. Data points on an IDF curve are usually derived from many segments of longer storms, and the values extrapolated by frequency analysis. It can be seen that the intensity of rainfall tends to decrease with increasing duration of rainfall for each of the IDF

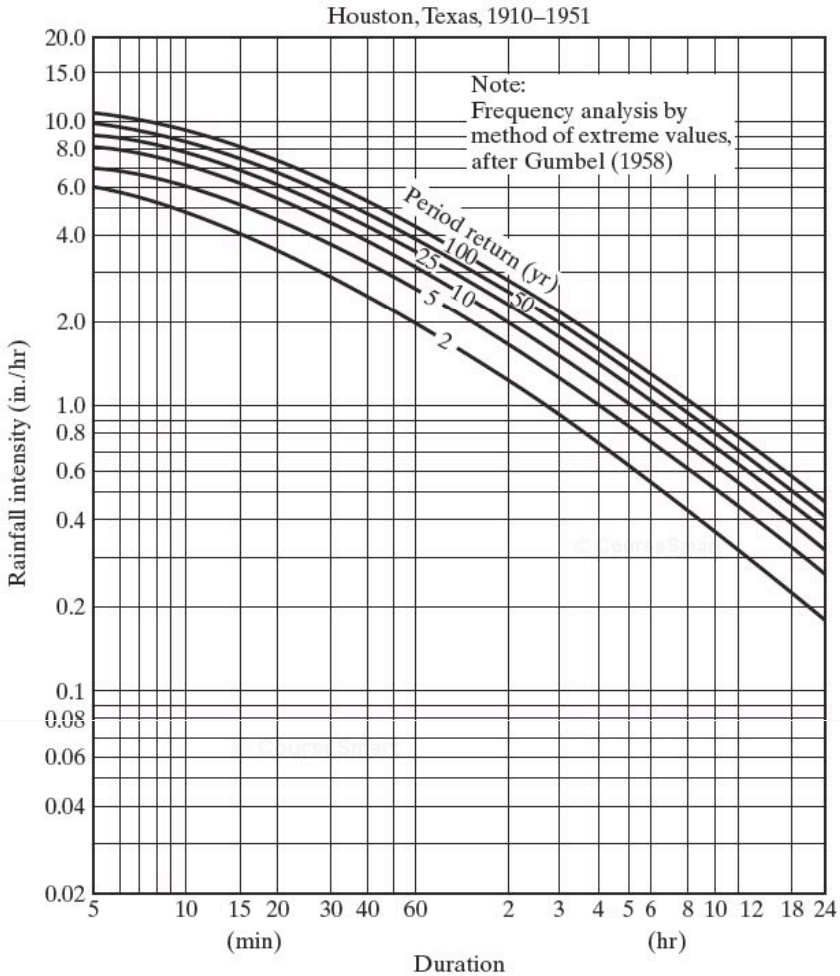

Figure 1–8
Intensity-duration-frequency curves for Houston, Texas.

curves. Instead of analyzing historical rainfall time series, the IDF curves can be used to derive design rainfall events, such as the 10-yr, 2-hr storm, which equals 2.0 in./hr, or the 10-yr, 24-hr storm, which equals 0.3 in./hr or 7.2 in. in 24 hr. One of the homework problems indicates how this procedure is carried out. Such design storms are often used as input to a hydrologic model for drainage design or flood analysis (see Chapters 5 and 6).

It is sometimes necessary to estimate point rainfall at a given location from recorded values at surrounding sites. The NWS (1972) has developed a method for this based on a weighted average of surrounding values. The weights are reciprocals of the sum of squares of distances D, measured from the point of interest. Thus,

$$D^2 = x^2 + y^2, \tag{1–8}$$

$$W = 1/D^2 = \text{weight}, \tag{1–9}$$

$$\text{rainfall estimate} = \sum_i P_i W_i / \sum_i W_i. \tag{1–10}$$

Areal Precipitation

Predicting watershed response to a given precipitation event often requires knowledge of the average rainfall that occurs over a watershed area in a specified duration. The average depth of precipitation over a specific watershed area is more accurately estimated for an area that is well monitored. Three basic methods exist to derive areally averaged values from point rainfall data: the arithmetic mean, the Thiessen polygon method, and the isohyetal method. Radar-based estimates of rainfall provide an interesting alternative for areas where rainfall gages may be lacking, and these methods are described in Chapter 11.

The simplest method is an arithmetic mean of point rainfalls from available gages [Fig. 1–9(a)]. This method is satisfactory if the gages are uniformly distributed and individual variations are not far from the mean rainfall. The method is not particularly accurate for larger areas where rainfall distribution is variable.

The **Thiessen polygon method** [Fig. 1–9(b)] allows for areal weighting of rainfall from each gage. Such a polygon is the locus of points closer to the

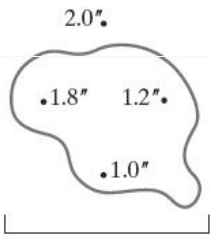

$$\frac{1.8 + 1.2 + 1.0}{3} = 1.33 \text{ in.}$$

(a) Arithmetic mean

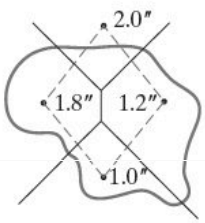

P_i (in.)	A_i (mi^2)	A_i/A_r	$(P_i)(A_i/A_r)$ (in.)
2.0	1.5	0.064	0.13
1.8	7.2	0.305	0.55
1.2	5.1	0.216	0.26
1.0	9.8	0.415	0.42
Σ =	23.6	1.000	1.35 in.

(b) Thiessen polygon method

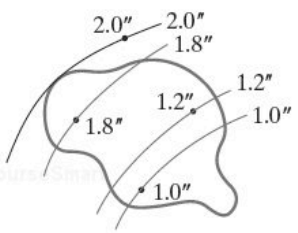

Isohyet (in.)	A (mi^2)	P_{av} (in.)	V (in.$-$mi^2)
2.0	5.1	1.9	9.69
1.8	9.8	1.5	14.7
1.2	3.1	1.1	3.41
1.0	5.6	0.5*	2.8
	23.6		30.6

Average rainfall = 30.6/23.6 = 1.30 in.

* Estimated

(c) Isohyetal method

Figure 1–9
Rainfall averaging methods.

given gage than to any other. Connecting lines are drawn between stations located on a map. Perpendicular bisectors are drawn to form polygons around each gage, and the ratio of the area of each polygon A_i within the watershed boundary to the total area A_T is used to weight each station's rainfall. The method is unique for each gage network and does not allow for orographic effects (those due to elevation changes), but it is probably the most widely used of the three available methods.

The **isohyetal method** [Fig. 1–9(c)] involves drawing contours of equal precipitation (isohyets) and is the most accurate method. However, an extensive gage network is required to draw isohyets accurately. The rainfall calculation is based on finding the average rainfall between each pair of contours, multiplying by the area between them, totaling these products, and dividing by the total area. The isohyetal method can include orographic effects and storm morphology and can represent an accurate map of the rainfall pattern, as shown for T. S. Allison in Houston [see Fig. 1–6(b)].

EXAMPLE 1–4 **RAINFALL AVERAGING METHODS**

A watershed covering 28.16 mi^2 has a system of seven rainfall gages, as shown on the map in Fig. E1–4(a). Using the total storm rainfall depths given in the accompanying table, determine the average rainfall over the watershed using (a) arithmetic averaging and (b) the Thiessen polygon method.

Gage	Rainfall (in.)
A	5.13
B	6.74
C	9.00
D	6.01
E	5.56
F	4.98
G	4.55

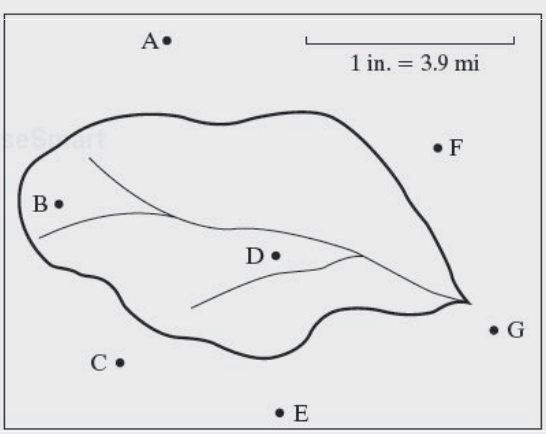

Figure E1–4(a)

SOLUTION

(a) For the arithmetic averaging method, only the gages within the watershed are used—in this example the gages B and D. Thus the arithmetic average is

$$(6.74 + 6.01)/2 = 6.38 \text{ in.}$$

(b) The first step in the Thiessen polygon method is to connect all nearby rain gages by straight lines. The result is a system of triangles, as shown by the dashed lines in Fig. E1–4(b). Next, we construct perpendicular bisectors of the dashed lines Fig. E1–4(c). The bisectors meet at a common point inside or outside the triangle. The resulting polygons around each rainfall gage are known as the Thiessen polygons.

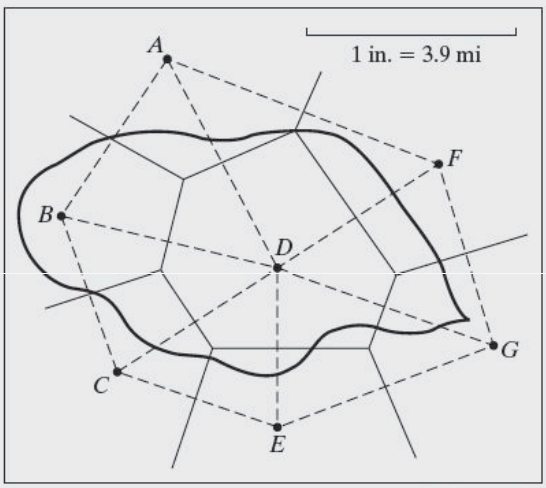

Figure E1–4(b)

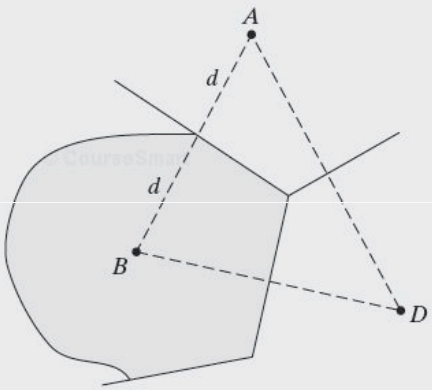

Figure E1–4(c)

The area of each polygon within the watershed boundary is measured using a map tool or GIS, or by counting squares on graph paper, and each individual area is divided by the total watershed area and multiplied by the depth of rainfall, measured at its corresponding gage. The sum of fraction area times rainfall for all the gages gives the average rainfall over the watershed. These computations, easily carried out in Microsoft Excel, are shown in the following table. A perpendicular bisector separates the triangle legs into two equal length segments. It intersects the leg at a 90-degree angle. The Thiessen polygons that weight each rain gage are created by the solid perpendicular bisector lines and the boundary of the watershed.

Thus, the Thiessen polygon method gives an average rainfall over the basin of

6.13 in., compared to 6.38 in. above

Table E1–4.

Gage	P_i (in.)	A_i (mi^2)	A_i/A_τ	$(P_i)(A_i/A_\tau)$ (in.)
A	5.13	1.74	0.062	0.32
B	6.74	6.70	0.238	1.60
C	9.00	1.77	0.063	0.57
D	6.01	13.02	0.463	2.78
E	5.56	0.83	0.029	0.16
F	4.98	2.68	0.095	0.47
G	4.55	1.42	0.050	0.23
		28.16	1.000	6.13

Radar-Based Precipitation

Advances in weather radar (called **NEXRAD** for next-generation radar) in the early 1990s greatly improved our ability to determine rainfall rates over watershed areas. The WSR-88D system is the Doppler weather radar originally deployed in a joint effort by the Departments of Commerce, Defense, and Transportation since 1992 (Crum and Alberty, 1993). NEXRAD is a 10-cm-wavelength radar that records reflectivity, radial velocity, and spectrum width of reflected signals. The radar is a volume-scanning radar, meaning that it employs successive tilt angles to cover an entire volume of the atmosphere and can measure reflectivity up to a range of 230 km. Depending on the current weather conditions, a specific volume coverage pattern (VCP) is used that varies the number of revolutions per tilt angle, and therefore varies the length of each complete volume scan. A more complete description of these and the other meteorological data products and processing may be found in Chapter 11 and in Crum and Alberty (1993), Klazura and Imy (1993), Smith et al. (1996), Fulton et al. (1998), and Vieux (2004).

Until the advent of the NEXRAD system nationwide, gaging stations were the only source of rainfall data for hydrologic modeling and flood prediction. Gage data are usually areally weighted, as described earlier, using Thiessen polygons or the isohyetal method, which assigns a rainfall distribution to a specific area associated with a point measurement. Archive level II radar data can be translated from their original radial coordinates into a gridded coordinate system with 1.0-km^2 resolution. Fulton et al. (1998) and Smith et al. (1996) both provide a description of radar applications and errors associated with precipitation estimates derived from reflectivity. Recent efforts have been successful in measuring rainfall rates and cumulative totals using radar technology developed and implemented in the 1990s (Vieux and Bedient, 1998; Bedient et al., 2000; Bedient et al., 2003; Vieux, 2004). Figure 1–10 depicts the type of radar rainfall information available from NEXRAD radar systems every 5–6 minutes for a storm event in Louisiana. Chapter 11 presents the background and details for using radar data to support hydro-

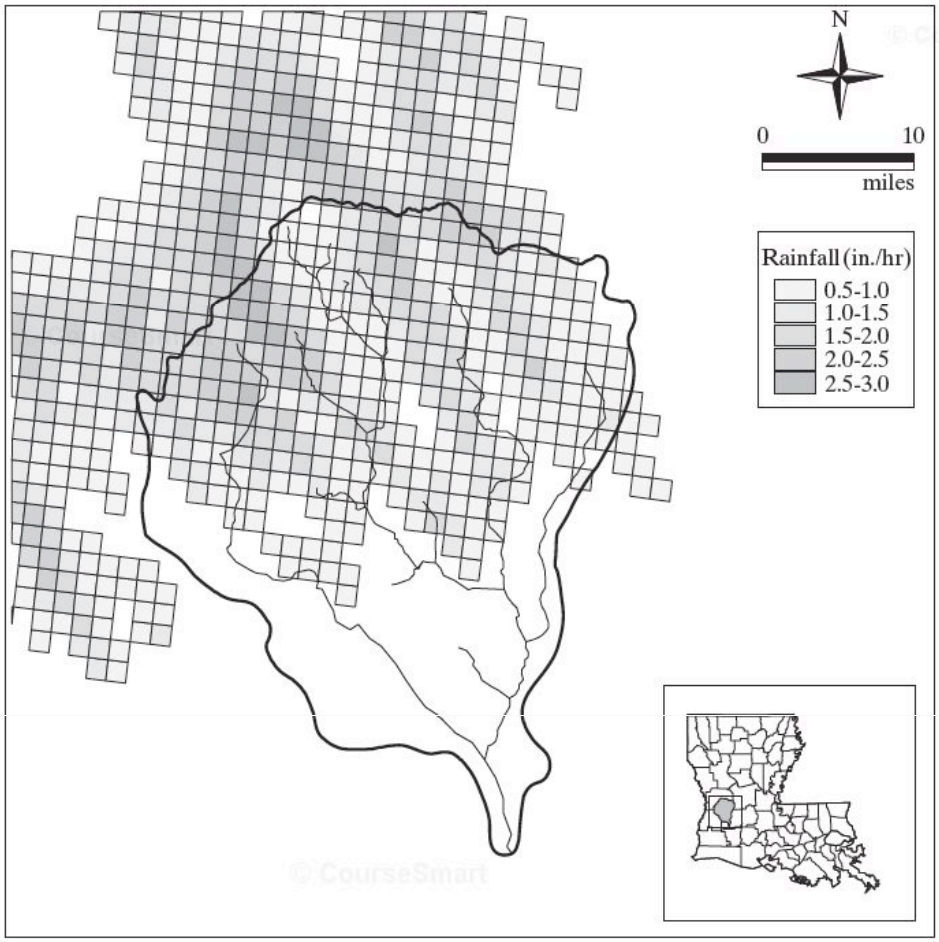

Figure 1–10
Typical NEXRAD radar rainfall data.

logic prediction from models and for associated flood alert systems. In addition, cumulative totals for any given grid location or for the entire watershed area can be easily obtained.

1.5 STREAMFLOW AND THE HYDROGRAPH

The hydrologic cycle is shown as a schematic in Fig. 1–1, where precipitation P initially falls on the land surface, and it may distribute to fill **depression storage**, infiltrate to become soil moisture and shallow ground water, or travel as interflow to a receiving stream. Evaporation E is often a small component of a specific storm event, since it is minimal as rain is actually falling, and is usually only a factor in longer-term water balances. Depression storage capacity is usually satisfied early in storm passage, followed by infiltration capacity (see Fig. 1–11). Eventually, overland flow and surface runoff commence after soil storage and depression storage are satisfied. The **hydrograph**, a plot of flow rate vs. time that is measured at a stream cross section, is made up